

University of Warwick institutional repository: <http://go.warwick.ac.uk/wrap>

This paper is made available online in accordance with publisher policies. Please scroll down to view the document itself. Please refer to the repository record for this item and our policy information available from the repository home page for further information.

To see the final version of this paper please visit the publisher's website. Access to the published version may require a subscription.

Author(s): Ladds G, Allen S, Moore K, Marsden C, Fulup V, Lord M, Roberts L and Kevin G Moffat

Article Title: The Isolation and Characterisation of Temperature Sensitive Ricin A Chain Molecules in *Saccharomyces cerevisiae*

Year of publication: 2007

Link to published version: <http://dx.doi.org/10.1111/j.1742-4658.2007.06080.x>

Title

The Isolation and Characterisation of Temperature-Dependent Ricin A Chain Molecules in *Saccharomyces cerevisiae*.

Stuart C. H. Allen¹, Katherine A. H. Moore¹, Catherine J. Marsden¹, Vilmos Fülöp¹, Kevin G. Moffat¹, J. Michael Lord¹, Graham Ladds² and Lynne M. Roberts¹.

¹ Department of Biological Sciences, University of Warwick, Coventry CV4 7AL, UK.

² Division of Clinical Sciences, Warwick Medical School, University of Warwick, UK.
CV4 7AL

Running title: Temperature-dependent ricin A chain mutants

Subdivision: Molecular Cell Biology

Corresponding author: L. M. Roberts, Department of Biological Sciences, University of Warwick, Coventry CV4 7AL, UK. Telephone: +44 (0)2476 523558. Fax: +44 (0)2476 523568. E-mail: Lynne.Roberts@warwick.ac.uk

Abbreviations: Endo H, endoglycosidase H; ER, endoplasmic reticulum; ERAD, endoplasmic reticulum associated degradation; Kar2_{SP}, Kar2p signal peptide; RTA, ricin toxin A chain; RTB, ricin toxin B chain.

Key words: ricin A chain; yeast; toxin; temperature-dependent mutants

Summary

Ricin is a heterodimeric plant protein that is potently toxic to mammalian cells. Toxicity results from the catalytic depurination of eukaryotic ribosomes by ricin A chain (RTA) that follows toxin endocytosis to, and translocation across, the endoplasmic reticulum (ER) membrane. To ultimately identify proteins required for these later steps in the entry process, it will be useful to express the catalytic subunit within the ER of yeast cells in a manner that initially permits cell growth. A subsequent switch in conditions to provoke innate toxin action would permit only those strains containing defects in genes normally essential for toxin retro-translocation, refolding or degradation to survive. As a route to such a screen, several RTA mutants with reduced catalytic activity have previously been isolated. Here we report the use of *Saccharomyces cerevisiae* to isolate temperature-dependent mutants of endoplasmic reticulum-targeted RTA. Two such toxin mutants with opposing phenotypes were isolated. One mutant RTA (RTA_{F108L/L151P}) allowed the yeast cells that express it to grow at 37°C while the same cells did not grow at 23°C. Both mutations were required for temperature-dependent growth. The second toxin mutant (RTA_{E177D}) allowed cells to grow at 23°C but not at 37°C. Interestingly, RTA_{E177D} has been previously reported to have reduced catalytic activity, but this is the first demonstration of a temperature-sensitive phenotype. To provide a more detailed characterisation of these mutants we have investigated their *N*-glycosylation, stability, catalytic activity and, where appropriate, a three dimensional structure. The potential utility of these mutants is discussed.

Introduction

Ricin A chain (RTA) is the catalytic polypeptide of the heterodimeric toxin ricin, which is produced in the endosperm of the seed of the castor bean plant, *Ricinus communis*. The study of ricin, in particular its route into target cells and the fate of its two subunits, RTA and the cell-binding galactose-specific lectin ricin B chain (RTB), are essential to gain further insights into the mechanism of toxin action [1].

During intoxication of mammalian cells, ricin is endocytosed to the endoplasmic reticulum (ER) from where the newly reduced A chain is retro-translocated to the cytosol [2-6]. The mechanism by which the RTA subunit is retro-translocated has not been fully elucidated but is thought to require at least some of the proteins involved in the branch of ER quality control that normally deals with misfolded/conformationally regulated proteins. These latter are detected, exported from the ER and degraded by proteasomes in a tightly coupled process known as ER-associated degradation (ERAD). It appears likely that RTA (and other toxins that reach the ER lumen) may hi-jack components of the ERAD pathway to reach the cytosol where a proportion of toxin can refold to a catalytically-active conformation [6-8]. The refolded fraction then removes a single adenine residue from the critical sarcin/ricin loop sequence of the 28S, 26S or 25S RNA (rRNA) of eukaryotic ribosomes [9]. This modification irreversibly disrupts the elongation factor-2 (EF-2) binding site [10], efficiently inhibiting protein synthesis. It is unclear at present whether this leads directly to cell death or whether ribotoxic stress ultimately triggers signal transduction leading to apoptosis [11, 12].

The budding yeast *Saccharomyces cerevisiae* has been used to study various cellular mechanisms, and the genetic tractability and ease of culturing has obvious advantages in genetic screens for mutant RTA open reading frames (ORFs) [13-15]. Although *Sc. cerevisiae* 25S rRNA molecules are very sensitive to RTA, yeast cells are not susceptible to externally administered ricin since they lack galactosyl transferase [16]. Thus they lack the galactosylated receptors needed to permit ricin uptake (as mentioned above, ricin is a galactose-specific lectin [17]). It is, however, possible to mimic the final stage in the intoxication process in yeast by directing RTA to the ER using a yeast (in this case, Kar2p) signal peptide (Kar2_{SP}) [7]. Using this targeted delivery approach we have already excluded some components of the yeast ERAD pathway as being important for RTA intoxication whilst implicating others [7].

To gain a more complete inventory of factors required for the entry of ricin A chain to the cytosol it will be useful to express inducible toxin in the ER of mutant strains of yeast, in a manner akin to its expression in plant cells [18]. Survivors of toxin expression may contain defects in genes normally essential for toxin retro-translocation, refolding, degradation or action on ribosomes. Such screens normally require the transformation of yeast libraries with plasmids encoding native ricin A chain whose expression is very tightly regulated. An alternative approach that avoids the need for stringent promoter regulation is the use of toxin variants whose effects on yeast cell growth can be controlled by a simple shift in temperature. In a previous study we have utilized the sensitivity of yeast cells to identify a number of RTA mutants with reduced catalytic activity [15]. Here, we describe the characterisation of a further class of RTA mutants in which the toxins expressed in yeast cells display cold-sensitive and heat-sensitive phenotypes. We believe

these temperature-dependent RTA mutants will be useful additions to the range of reagents that can be used in future genetic screens aimed toward identifying yeast components required for ER retro-translocation and cytosolic refolding of ricin.

Results

We used a vector-based RTA ORF fused to the co-translational Kar2p signal sequence (Kar2_{SP}) in order to isolate attenuated RTA molecules that had been directed to the ER lumen. Figure 1 shows a schematic that depicts the procedure for gap repair cloning and the selection of temperature-dependent mutants. The gap repair transformation was performed using *Bgl*III cut pRS316 Kar2_{SP}-RTA as the vector together with the product from 5 rounds of error prone, *Taq* polymerase-based PCR of the entire RTA ORF (see Materials and Methods, and Allen *et al.*, [15]). Yeast were plated onto selective media at either 37°C or 23°C respectively and allowed to grow for 16 hours before they were replica plated and grown at alternative temperatures (23°C or 37°C respectively). Isolates growing at both temperatures were ignored whilst isolates growing only at one of the temperatures (termed permissive, where the expression of toxin did not inhibit cell growth) were picked and further screened. To further analyse these isolates, plasmid DNA was extracted, purified and sequenced to determine the nature of the mutations. Any mutations discovered were remade in the wild-type Kar2_{SP}-RTA plasmid before re-testing and validating the effects on cell growth by transforming W303.1C and plating the cells at 23°C, 30°C and 37°C.

A cold-sensitive growth phenotype (where toxin is active and interferes with cell growth only at low temperature) was isolated from cells expressing RTA in which Phe108 was converted to Leu (specified by the point mutation T322C), and Leu151 was converted to Pro (specified by the point mutation T452C). Base numbers relate to the published RTA coding sequence [19]. These two amino acid substitutions were individually introduced

into a wild-type RTA plasmid but temperature-dependent growth of transformants was no longer observed (Fig. 2A). In contrast, a heat-sensitive growth phenotype (where toxin is active and interferes with cell growth only at a high temperature) was isolated from cells expressing RTA with point mutation A531 to C, which converted the active site Glu177 to Asp (Fig. 2A). This particular mutant (RTA_{E177D}) has previously been described as having reduced catalytic activity [13, 20], although its temperature-dependence was not investigated. To confirm that yeast cells were able to grow at all temperatures when expressing a known inactive RTA variant, Kar2_{SP}-RTA Δ was utilized in which key active site residues are missing [7]. Interestingly, when the double mutant is expressed in the cytosol without a signal peptide, the yeast cells grow at 37°C only (Fig. 2B). The growth pattern is similar to that of RTA_{F108L/L151P} when targeted to the ER (Fig. 2A) although no growth is ever observed at 30°C. This demonstrates that the cold-sensitive growth phenotype seen in this yeast strain genuinely reflects of the sensitivity of the mutant toxin to temperature.

To obtain a clearer picture of the growth profiles of yeast cells expressing these RTAs, cells were plated at various temperatures as illustrated in Figure 3A. Yeast cells expressing Kar2_{SP}-RTA_{F108L/L151P} were unable to grow at temperatures below 25°C. For cells expressing Kar2_{SP}-RTA_{E177D}, growth was observed at all temperatures with the exception of 37°C. In contrast, the Kar2_{SP}-RTA Δ variant showed comparable growth at all temperatures. The growth profiles of Kar2_{SP}-RTA_{E177D} at 30°C and 37°C, and Kar2_{SP}-RTA_{F108L/L151P} at 23°C and 37°C, were validated in liquid cultures with time courses confirming the predicted phenotypes (Fig. 3B). However, neither of the temperature-dependent RTA variants was lethal since the cells expressing them were fully viable

when returned to the respective permissive temperature (Fig. 3C). Indeed, when RTA-expressing cells were maintained at temperatures restrictive for growth for more than 72 hours, they were fully viable when shifted back to the respective permissive temperature (data not shown).

We next sought to determine the *in vivo* catalytic activities (i.e. the ability to depurinate 25S rRNA of yeast ribosomes) of the RTA_{E177D} and RTA_{F108L/L151P} variants at various temperatures. Yeast cells expressing either Kar2_{SP}-RTA_{E177D} or Kar2_{SP}-RTA_{F108L/L151P} were grown for approximately 24 hours at the permissive temperatures of 30°C and 37°C, respectively. A sample of the cells was removed from each culture, rRNAs were isolated in Trizol, and the extent to which they had been depurinated by active toxin *in vivo* determined (this is designated as time 0 in Fig. 4). The remainder of each culture was divided into two, with one half being incubated at the permissive temperature for a further 24 hours while the other half was incubated at the non-permissive temperature for the same period. Toxin-mediated damage to ribosomes renders the depurinated site highly labile to hydrolysis by acetic-aniline. Therefore, each sample of isolated rRNA was treated with acetic-aniline and separated on a denaturing gel before blotting to detect any hydrolysed rRNA fragments (see Methods; [20]). As shown in Figure 4, ribosomes isolated from yeast grown at the permissive temperature or from yeast incubated for a further 24 hours at the permissive temperature revealed a lower level of rRNA depurination than cells grown at the non-permissive temperature. This demonstrates that the expressed RTAs are more biologically active in yeast at the temperatures non-permissive for growth, supporting the notion that rRNA depurination, if sufficiently high enough, affects cell growth.

N-glycosylation provides evidence that RTA enters the ER lumen. Native RTA contains two *N*-glycosylation sites [19] although only one of these sites is usually used [21]. The extent of *N*-glycosylation of RTA Δ , RTA_{F108L/L151P} and RTA_{E177D} variants was determined. After incubation of cells expressing the RTA mutants at the permissive temperatures, they were radiolabelled for 20 minutes at 23°C, 30°C and 37°C. Following cell lysis and immunoprecipitation, labelled RTA moieties were visualised by fluorography after SDS-PAGE. Figure 5 shows that the different RTA variants were indeed expressed at all temperatures and that they efficiently reached the ER lumen, as judged by glycosylation and signal peptide removal. Digestion with Endoglycosidase H (Endo H) confirmed that the higher molecular weight forms were *N*-glycosylated. RTA Δ , which is completely devoid of catalytic activity, was more extensively *N*-glycosylated than RTA_{E177D}, most likely because RTA Δ cannot fold correctly, prolonging exposure of its glycosylation sequons to oligosaccharyl transferase. Interestingly RTA_{F108L/L151P}, which retains some catalytic activity at the temperature permissive for cell growth, displayed a similar *N*-glycosylation profile to RTA Δ , again indicating some difficulty in assuming a tightly folded conformation. By contrast, RTA_{E177D} is mainly non glycosylated with only a minor fraction carrying a single glycan. This is more typical of a toxin that rapidly assumes its folded conformation (our unpublished observations). The deglycosylated RTAs (Fig. 5, + Endo H lanes) had the same gel mobility as the *in vitro* translated control that lacked a signal peptide. There is no evidence of a slower migrating, signal peptide-uncleaved RTA in the glycosidase-treated samples, demonstrating efficient ER delivery and subsequent signal peptide cleavage.

We next determined the stabilities of ER-delivered RTA_{E177D} and RTA_{F108L/L151P} as a function of temperature. Cells expressing the variants were pulse-labelled for 20 minutes with [³⁵S]-Promix, and chased for up to 30 minutes (Fig. 6A). The analysis of RTA_{E177D} agrees with previously published data with respect to its disappearance at 30°C, and is consistent with the retro-translocation of this protein to the cytosol where a proportion is degraded by proteasomes [7]. Although more protein is synthesised during the short pulse at 37°C (Fig 6A; 37°C, zero chase point), it is evident that some protein turnover occurred at all the temperatures assayed (Fig. 6A). In contrast, visual inspection revealed that retro-translocated RTA_{F108L/L151P} disappeared most markedly at 23°C while it appeared completely stable at 37°C (Fig. 6B). Stability was observed at the higher temperature when this protein was expressed either by the ER lumen or directly in the cytosol without a signal peptide. Such apparent stability may provide an explanation as to why yeast cells can tolerate expression and persistence of this protein under these conditions, as it may misfold at the higher temperature to yield an inactive, protease-resistant aggregate.

We attempted to obtain the X-ray crystallographic structures of the temperature-dependent RTA variants. Despite repeated attempts using *Escherichia coli* as the expression host at a variety of temperatures, we were unable to purify the necessary amount of RTA_{F108L/L151P}. By contrast, recombinant RTA_{E177D} was readily purified from bacteria and shown to depurinate yeast ribosomes *in vitro* when assayed at either 30°C or 37°C. Figure 7A shows denaturing gels of aniline-treated rRNA extracted from purified yeast ribosomes that had been treated with decreasing doses of RTA_{E177D} at 30°C and 37°C. Acetic-aniline will only hydrolyse the phosphoester bond at a depurinated site

(such as the site in rRNA that becomes modified by toxin). This releases a small fragment of 25S rRNA that is readily visible on gels, migrating between the larger and smaller intact rRNA species. The released fragments were quantified relative to 5.8S rRNA to control for differences in gel loading, and the percentage of depurinated rRNA was determined at different RTA_{E177D} concentrations [20]. Not unexpectedly, at low RTA_{E177D} concentrations, the rate of depurination was faster at 37°C than at 30°C (Fig. 7B). The *in vitro* DC₅₀ (the amount of protein required to depurinate 50% of the ribosomes) also decreased with temperature from 486ng at 30°C to 209ng at 37°C. This increased depurination at higher temperatures would explain the inability of yeast cells expressing RTA_{E177D} to grow at 37°C.

Purified recombinant RTA_{E177D} was crystallised and its structure determined (Fig. 8). Compared to wild-type RTA, the E177D mutation resulted in a side-chain shortened by a methylene group, which slightly altered the position of the salt-bridged Arg180. This subtle conformational change disrupts the close contact between Arg180 and Tyr80 observed in the wild-type structure, forcing the Tyr80 side-chain to move slightly leaving it more exposed to solvent and breaking the hydrogen bond between the hydroxyl group of Tyr80 and the Gly121 carbonyl oxygen (Fig. 8, compare A and B with C). These changes are very slight but since they involve active site residues, they impact on toxin activity. In our first experiment we followed the optimized crystallisation conditions of Weston *et al.* [22], which resulted in an acetate ion bound (salt-bridged) to Arg180 and sandwiched between the aromatic rings of Tyr80 and Tyr123 close to the single point mutation site of E177D (Fig. 8A). We then replaced acetate in the crystallisation mother liquor with citrate, which gave a virtually identical side-chain arrangement surrounding

the mutation site (Fig. 8B). The structure of the RTA_{E177D} mutant is essentially identical to that of recombinant wild-type RTA with a root mean square deviation (RMSD) from the C α atoms of the wild-type crystal structure [22] of 0.33 Å. The electron density in the area local to the substitution is shown in Fig. 8, A and B. Figure 8 D shows a ribbon diagram of wild-type RTA structure and the positions of the altered amino acids of the double mutant, F108 and L151, within the structure are indicated.

Discussion

RTA is the catalytic polypeptide of the heterodimeric toxin ricin. After binding to target mammalian cells, ricin is endocytosed to the ER lumen where toxin reduction and subunit retro-translocation to the cytosol occurs. This reverse translocation is believed to require an unfolded/partially folded protein that, in the case of RTA, may occur through exposure of a C-terminal hydrophobic domain upon reduction. On the cytosolic side of the membrane, a proportion of RTA must refold so that it can inactivate ribosomes by depurination [10]. Ribosomes modified in this way are no longer capable of synthesising proteins, and when an appropriate proportion of the total cellular ribosome pool has been depurinated, protein synthesis is insufficient for viability leading either directly to cell death or by triggering apoptotic pathways. Although much is known about the trafficking of toxins, a lot less is known about these downstream steps of cell intoxication. Experimental evidence pertinent to this question is patchy at present, but the emerging picture indicates that toxins like ricin can exploit an unknown number of ER and membrane components normally involved in perceiving and extracting proteins from the ER to the cytosol [23]. In order to ultimately identify the complete repertoire of molecules involved, we have generated and characterised two temperature-dependent RTA mutants from yeast. These will be utilized in subsequent screens for yeast genes important for the cytosolic entry of ricin A chain.

We have previously reported a novel mechanism for gap repair cloning in *Sc. cerevisiae* that can be used to generate mutations only within the RTA ORF. These mutations frequently resulted in attenuated toxins [15]. Here we have extended this strategy to screen for toxins whose activity was altered at different temperatures. In this way, we

have isolated RTA_{F108L/L151P} that permits cells to grow only above 25°C and RTA_{E177D}, that permits cell growth at all but 37°C. Upon constitutive, plasmid-driven expression, both toxins were efficiently delivered to the ER lumen by the signal peptide of Kar2p. This was verified by the detection of either glycosylated or non-glycosylated but signal peptide-cleaved forms (Fig. 5). Subsequent retro-translocation of these RTAs would be predicted to result in ribosome modification, which if excessive, would lead to cell intoxication and death. However, the precise outcome would depend on a number of factors, not least the available pool of unmodified ribosomes.

Yeast cells shifted to higher temperatures may have a smaller population of ribosomes. Indeed, it has been reported that yeast cells switched to 37°C show a dramatic decrease in ribosomal protein transcription within the first 20 minutes. However, the normal rate of ribosome synthesis is resumed within the hour [24, 25]. We therefore postulate that the reduced ability of yeast to grow whilst remaining viable after incubation at 37°C, is not simply a reflection of a smaller pool of ribosomes. However, the balance between the number of functional ribosomes required for cells to grow and the number of ribosomes inactivated by toxin must be critical. We deduce that when cells expressing RTA_{E177D} are incubated at 37°C, more RTA protein is made (Fig. 5) and the enzyme is sufficiently active (Fig. 4) to depurinate enough ribosomes to inhibit cell growth (Fig. 2A). However, in contrast to the lethality observed with native RTA [15], it is important to reiterate that cells expressing RTA_{E177D} at 37°C remain viable and resume growth when returned to a lower temperature (Fig. 3C), supporting the contention that in this case, it is the proportion of active ribosomes required for growth that is critical. Indeed, Gould *et al.*, [14] reported that yeast could tolerate ~20% ribosome inactivation, while the present

study indicates that in the yeast strain used here, only a depurination level greater than ~35% was detrimental and prevented growth (Fig. 4). It should be noted that the mechanism of growth arrest seen here is not known with certainty.

RTA_{E177D} has previously been shown to be ~50-fold less catalytically active than wild-type RTA [20]. As such, it is often used in experiments where the toxin needs to be visualised in the absence of cell death [18, 21, 26]. In an attempt to establish a structural basis for this reduction in activity, we have now solved the X-ray crystallographic structure of RTA_{E177D} to 1.6Å resolution. A comparison of the mutant RTA structure with that of wild-type RTA [22] shows that the two structures are essentially identical apart from some subtle side-chain realignments in the region of the active site (Fig. 8). These realignments in RTA_{E177D} must account for its reduced catalytic activity. However, it is important to note that the structure is essentially native. This finding will be particularly pertinent for studies of RTA retro-translocation where a protein with reduced activity but with as near native a structure as normal is required. The solved structure of RTA_{E177D} will deflect concerns that a mutant, and by inference a structurally-defective variant, is being used to probe events relating to the behaviour of a native polypeptide.

The novel RTA_{F108L/L151P} isolated in the present study allows yeast to grow above ~25°C but not at lower temperatures (Figs. 3A and B). However, significantly less RTA_{F108L/L151P} was produced at 23°C - when the cells failed to grow, than at 37°C when cells grew normally (Fig. 5 and Fig. 6B zero chase points). We propose that the most likely explanation for this curious observation is that while ER-targeted RTA_{F108L/L151P} retro-translocates to the cytosol at 23°C where a fraction can damage ribosomes even

though the bulk will be targeted for proteasomal degradation, this mutant toxin aggregates at 37°C to a non-active, protease-resistant species. Consistent with this, upon pulse-chase, both glycosylated and non glycosylated RTA_{F108L/L151} appeared completely stable at 37°C, in contrast to their behaviour at lower temperatures (Fig. 6B). Cells expressing a version without an ER signal peptide also grew at 37°C (Fig. 2B) and the cytosolic protein similarly persisted with time at this temperature (Fig.6B; cRTA_{F108L/L151P}), indicating a general (rather than an ER-specific) propensity to misfold, aggregate and resist turnover at the higher temperature.

We report that RTA_{F108L/L151P} required both substitutions for yeast cells to exhibit temperature-dependent growth. RTAs carrying the equivalent single amino acid substitutions behaved like wild type RTA in that transformed cells failed to grow at any of the temperatures tested (Fig. 2A). In contrast, when both point mutations were simultaneously introduced into a wild type RTA ORF, transformants were once again cold-sensitive for growth. We attempted to obtain the X-ray crystallographic structures of the single and double RTA_{F108L/L151P}, but repeatedly failed to purify appropriate amounts following expression in *E. coli*. It is possible this protein has a tendency to be unstable in *E. coli* and hence is difficult to express in large amounts. Some difficulty in assuming a folded conformation is indicated by the *N*-glycosylation pattern of this protein in yeast (Fig. 5, compare the glycan pattern of RTA_{F108L/L151P} with the efficiently glycosylated but misfolded RTA Δ and the under-glycosylated but near-native RTA_{E177D}) and the finding of an apparently stable (we propose, aggregated) species when expressed in yeast at the higher temperature. Nevertheless, there is clearly activity associated with RTA_{F108L/L151P},

which implies the protein can be folded correctly when it is expressed at temperatures below 28°C (Fig. 3A, Fig. 4B).

The striking switch of growth versus no growth observed when both RTA_{F108L/L151P} and RTA_{E177D} are expressed at different temperatures provides a simple and effective way of screening for yeast genes that perturb the cytosolic entry, degradation or refolding of ricin. Furthermore, it circumvents the need to use tightly regulated promoters to maintain cell growth in the presence of plasmids carrying a native RTA coding sequence to such time that induction of expression is required. Such promoters can be variously leaky, with consequent lethality when native ricin A chain is being made [14]. Although beyond the scope of the present study, it now remains for such proteins to be utilized in yeast genetic screens and for their behaviour to be fully characterised in mammalian and plant systems.

Experimental Procedures

Yeast strain, manipulations and growth media.

Cultures of *Sc. cerevisiae* strain W303.1C (*MATa ade2 his3 leu2 trp1 ura3 prc1*) were routinely grown in YPDA media (1% (w/v) yeast extract, 2% (w/v) peptone, 2% (w/v) glucose, 450 μ M adenine). W303.1C cells transformed with pRS316, a *CEN6/URA3* expression vector [27], were grown on solid synthetic complete drop out media lacking uracil (AA-ura) as previously described [7]. Yeast transformations were achieved by using the lithium acetate/single stranded DNA/PEG method as previously described [28]. The expression of Kar_{2SP}-RTA wild type and mutant ORFs from the pRS316 vectors was under the control of the *GAPDH* promoter and the *PHO5* terminator as previously described [7].

PCR mutagenesis.

RTA variants were generated by multiple rounds of error-prone PCR using *Taq* DNA polymerase (Invitrogen) as described previously [15]. Oligonucleotide primers used to amplify the mature ORF of RTA were CP172 5'-ATATTCCCCAAACAATACCC-3' and the antisense primer CP133 5'-**TTAA**AACTGTGACGATGGTGGGA-3' with the TAA termination anti-codon shown in bold. Amplification reactions were performed in a final volume of 50 μ l containing 5 ng of template DNA according to the manufacturer's instructions. The final PCR product was purified using a QIAquick Gel Extraction Kit (Qiagen) according to the manufacture's protocol, and quantified by determining the absorbance at 260 nm and used directly in yeast transformations.

Yeast plating.

Yeast cultures were grown overnight at the permissive temperatures in liquid media. To ensure an even number of colonies per plate, the cultures were diluted to 4×10^4 cells ml^{-1} , before 1×10^4 cells were plated onto AA-ura agar. Plates were incubated at the appropriate temperature for various times until colonies of similar sizes were formed.

Pulse-chase analyses.

Pulse-chase experiments were performed as described previously [7]. Briefly, 3.7×10^7 cells, grown at the permissive temperature, were washed and harvested before being starved of methionine for 30 minutes at either 30°C or 37°C. Cells were then incubated with 70 μCi of [^{35}S]-Promix (GE Healthcare, U.K.) at the respective temperatures for 20 minutes before the addition of excess unlabelled methionine and cysteine (met/cys) to start the chase. Chase samples were taken at time zero and various time points thereafter, and RTA immunoprecipitated from cell lysates as described previously [7].

Endoglycosidase H treatment.

Radiolabelled immunoprecipitates bound to Protein A-Sepharose beads were either resuspended in 40 μl Endo H buffer (0.25 M sodium citrate pH 5.5 and 0.2 % (w/v) SDS) or in SDS-polyacrylamide gel electrophoresis (PAGE) loading buffer [29] to a final volume of 30 μl . Pellets resuspended in Endo H buffer were heated at 95°C for 5 minutes, cooled and vortexed before pelleting the Protein A-Sepharose beads at 6000 g for 1 min. The supernatant was collected and split into two equal samples: to one was added 2 μl H_2O and to the other was added 2 μl Endo H (0.005U/ μl) (Roche). Samples were incubated at 37°C overnight before being adjusted to 1x PAGE loading buffer in a final

volume of 30 μ l. Samples were subjected to SDS-PAGE, and radioactive bands visualised by fluorography.

Plasmid DNA extraction from yeast.

Plasmids were isolated from yeast using the protocol described by Hoffman and Winston, [30]. Briefly, washed cells were lysed and nucleic acids extracted by phenol extraction and precipitated with ethanol. The nucleic acid pellet was re-suspended in distilled H₂O and competent *Escherichia coli* DH5 α (F'/*endA1 hsdR17*(r_K⁻m_K⁺) *supE44 thi*⁻¹ *recA1 gyrA* (Nal^r) *relA1 D(lacIZYA-argF)U169 deoR* (F80*dlacD(lacZ)M15*)) cells transformed. Plasmids were isolated from the resulting transformants and the DNA sequenced.

Expression and purification of recombinant RTA_{E177D}.

Recombinant RTA_{E177D} was purified from bacteria as described previously [31]. Briefly, a single colony of *E. coli* JM101 (F' *traD36 proA*⁺*B*⁺ *lacI*^f Δ (*lacZ*)*M15/* Δ (*lac-proAB*) *glnV thi*) transformed with the pUTA vector [32] containing the RTA_{E177D} sequence was used to inoculate 50 ml of 2YT (2% (w/v) peptone, 1% (w/v) yeast extract, 85 mM NaCl) and grown overnight at 37°C. This culture was used to inoculate 500 ml of 2YT, and the culture was grown for 2 h at 30°C. Expression was induced by adding isopropyl thio- β -D-galactoside to a final concentration of 0.1 mM for 4 h at 30°C. Cells were harvested by low speed centrifugation, resuspended in 15 ml of 5 mM sodium phosphate buffer (pH 6.5), and lysed by sonication on ice. Cell debris was pelleted by centrifugation at 31,400 *g* at 4°C for 30 min and the supernatant loaded onto a 50 ml CM-Sepharose CL-6B column (Amersham Biosciences). The column was washed with 1 l of 5 mM sodium phosphate (pH 6.5) followed by 100 ml of 100 mM NaCl in 5 mM sodium phosphate (pH 6.5) and

RTA_{E177D} was eluted with a linear gradient of 100–300 mM NaCl in the same buffer. Fractions containing RTA_{E177D} were pooled and stored at 4°C at a concentration of 1 mg/ml.

Crystallisation, X-ray data collection and refinement of RTA_{E177D}.

Crystals were grown in the tetragonal space group P41212 by the sitting-drop method using microbridges (Crystal Microsystems, UK) and the conditions described for wild-type RTA crystallisation [22] and also under conditions where citrate buffer was substituted for acetate buffer. Data were collected at 100 K using 15% (v/v) glycerol as a cryoprotectant and processed using the HKL suite of programs [33]. Refinement of the structures was carried out by alternate cycles of REFMAC [34] and manual refitting using O [35], based on the 1.8 Å resolution model of wild-type RTA [22] (Protein Data Bank code 1ift). Water molecules were added to the atomic model automatically using ARP [36] at the positions of large positive peaks in the difference electron density, only at places where the resulting water molecule fell into an appropriate hydrogen bonding environment. Restrained isotropic temperature factor refinements were carried out for each individual atom. Data collection and refinement statistics are given in Table 1.

RNA extraction.

Yeast cells expressing RTA were grown at either permissive or non-permissive temperatures before being harvested and resuspended in Trizol (Invitrogen) prior to lysis. RNA from 5×10^7 cells was extracted using standard techniques [37].

In vitro depurination of salt washed ribosomes.

Purified salt-washed yeast ribosomes (20 μ g) were treated with halving dilutions of purified RTA_{E177D} (starting at 250 ng/ μ l) in 25 mM Tris-HCl pH 7.6, 25 mM KCl, 5 mM MgCl₂ and 10 mM Ribonucleoside Vanadyl Complex (New England BioLabs, Inc.) for 1 hour at either 30 or 37°C. The reaction was stopped with the addition of 1x Kirby Buffer [38]. The rRNA was then extracted using phenol:chloroform (1:1 v/v) and precipitated with ethanol. 4 μ g of this isolated RNA was treated with 20 μ l of acetic-aniline pH 4.5 for 2 minutes at 60°C, precipitated using 0.1 volumes of 7M ammonium acetate and 2.5 volumes of 100% ethanol, and pelleted by centrifugation at 12,000 g for 30 minutes at 4°C. The pellets were washed with 1ml of 75% (v/v) ethanol prior to vacuum drying. RNA was resuspended in 20 μ l of 60% (v/v) formamide in 0.1xTPE (0.36 mM Tris HCL pH 8.0, 0.3 mM NaH₂PO₄, 0.01 mM EDTA) and electrophoresed on a denaturing formamide gel. RNA was then visualised after staining the gel with ethidium bromide on a GelDoc-it (UVP) imaging system, using LabWorks version 4.0.0.8 software (UVP). The RNA fragments resulting from aniline hydrolysis were quantified using TotalLab™, version 2003.02 (Nonlinear Dynamics Ltd). Depurination in each lane was calculated by relating the amount of any rRNA fragment released upon aniline treatment with the amount of 5.8S rRNA (directly proportional to the quantity of 25S rRNA) and expressing values as percentages, after correcting intensities according to rRNA size.

Northern blot analysis of depurinated rRNA.

Aniline treated rRNA was electrophoresed under denaturing conditions before being transferred to Hybond-N nitrocellulose membrane (Amersham) as per Sambrook *et al.*, [29]. RNA sequences were probed with a 422 base DNA probe with a sequence

homologous to the 3' end of the 25S rRNA DNA sequence. The probe template was amplified using oligonucleotides CP245 5'-GATCAGGCATTGCCGCGAAGC-3' and CP246 5'-GAGACTTGTTGAGTCTACTTC-3' from a plasmid DNA containing the 25S rRNA genomic DNA sequence. The probe was made by random priming and the incorporation of [α -³²P]dCTP. Hybridization of the probe to the membrane and subsequent washes were performed as described [29]. Hybridization was detected by autoradiography and specific hybridization to the aniline fragment was quantified using TotalLab™ version 2003.02.

Acknowledgments

This work was supported by a grant from the UK Department of Health (to LMR, JML, GL and KGM). GL is supported by the University Hospitals of Coventry and Warwickshire NHS Trust. We are grateful for access and user support at the synchrotron facilities at ESRF, Grenoble and MAXLAB, Lund. The authors would like to thank Dr J. P. Cook for *in vitro* transcription plasmids and Dr R. A. Spooner for critical reading of the manuscript.

References

1. Lord, M. J., Jolliffe, N. A., Marsden, C. J., Pateman, C. S., Smith, D. C., Spooner, R. A., Watson, P. D. & Roberts, L. M. (2003) Ricin. Mechanisms of cytotoxicity, *Toxicol Rev.* **22**, 53-64.
2. Wales, R., Roberts, L. M. & Lord, J. M. (1993) Addition of an endoplasmic reticulum retrieval sequence to ricin A chain significantly increases its cytotoxicity to mammalian cells, *J Biol Chem.* **268**, 23986-90.
3. Simpson, J. C., Dascher, C., Roberts, L. M., Lord, J. M. & Balch, W. E. (1995) Ricin cytotoxicity is sensitive to recycling between the endoplasmic reticulum and the Golgi complex, *J Biol Chem.* **270**, 20078-83.
4. Rapak, A., Falnes, P. O. & Olsnes, S. (1997) Retrograde transport of mutant ricin to the endoplasmic reticulum with subsequent translocation to cytosol, *Proc Natl Acad Sci U S A.* **94**, 3783-8.
5. Lord, J. M. & Roberts, L. M. (1998) Toxin entry: retrograde transport through the secretory pathway, *J Cell Biol.* **140**, 733-6.
6. Wesche, J., Rapak, A. & Olsnes, S. (1999) Dependence of ricin toxicity on translocation of the toxin A-chain from the endoplasmic reticulum to the cytosol, *J Biol Chem.* **274**, 34443-9.
7. Simpson, J. C., Roberts, L. M., Romisch, K., Davey, J., Wolf, D. H. & Lord, J. M. (1999) Ricin A chain utilises the endoplasmic reticulum-associated protein degradation pathway to enter the cytosol of yeast, *FEBS Lett.* **459**, 80-4.
8. Lord, J. M., Roberts, L. M. & Lencer, W. I. (2005) Entry of protein toxins into mammalian cells by crossing the endoplasmic reticulum membrane: co-opting basic mechanisms of endoplasmic reticulum-associated degradation, *Curr Top Microbiol Immunol.* **300**, 149-68.
9. Endo, Y., Mitsui, K., Motizuki, M. & Tsurugi, K. (1987) The mechanism of action of ricin and related toxic lectins on eukaryotic ribosomes. The site and the characteristics of the modification in 28 S ribosomal RNA caused by the toxins, *J Biol Chem.* **262**, 5908-12.
10. Moazed, D., Robertson, J. M. & Noller, H. F. (1988) Interaction of elongation factors EF-G and EF-Tu with a conserved loop in 23S RNA, *Nature.* **334**, 362-4.
11. Iordanov, M. S., Pribnow, D., Magun, J. L., Dinh, T. H., Pearson, J. A., Chen, S. L. & Magun, B. E. (1997) Ribotoxic stress response: activation of the stress-activated protein kinase JNK1 by inhibitors of the peptidyl transferase reaction and by sequence-specific RNA damage to the alpha-sarcin/ricin loop in the 28S rRNA, *Mol Cell Biol.* **17**, 3373-81.
12. Higuchi, S., Tamura, T. & Oda, T. (2003) Cross-talk between the pathways leading to the induction of apoptosis and the secretion of tumor necrosis factor-alpha in ricin-treated RAW 264.7 cells, *J Biochem (Tokyo).* **134**, 927-33.
13. Frankel, A., Schlossman, D., Welsh, P., Hertler, A., Withers, D. & Johnston, S. (1989) Selection and characterization of ricin toxin A-chain mutations in *Saccharomyces cerevisiae*, *Mol Cell Biol.* **9**, 415-20.
14. Gould, J. H., Hartley, M. R., Welsh, P. C., Hoshizaki, D. K., Frankel, A., Roberts, L. M. & Lord, J. M. (1991) Alteration of an amino acid residue outside the active site of the ricin A chain reduces its toxicity towards yeast ribosomes, *Mol Gen Genet.* **230**, 81-90.

15. Allen, S. C., Byron, A., Lord, J. M., Davey, J., Roberts, L. M. & Ladds, G. (2006) Utilisation of the budding yeast *Saccharomyces cerevisiae* for the generation and isolation of non-lethal ricin A chain variants., *Yeast*. 22, 1287-97.
16. Gemmill, T. R. & Trimble, R. B. (1999) Overview of N- and O-linked oligosaccharide structures found in various yeast species, *Biochim Biophys Acta*. 1426, 227-37.
17. Olsnes, S., Saltvedt, E. & Pihl, A. (1974) Isolation and comparison of galactose-binding lectins from *Abrus precatorius* and *Ricinus communis*, *J Biol Chem*. 249, 803-10.
18. Di Cola, A., Frigerio, L., Lord, J. M., Ceriotti, A. & Roberts, L. M. (2001) Ricin A chain without its partner B chain is degraded after retrotranslocation from the endoplasmic reticulum to the cytosol in plant cells, *Proc Natl Acad Sci U S A*. 98, 14726-31.
19. Lamb, F. I., Roberts, L. M. & Lord, J. M. (1985) Nucleotide sequence of cloned cDNA coding for preprorizin, *Eur J Biochem*. 148, 265-70.
20. Chaddock, J. A. & Roberts, L. M. (1993) Mutagenesis and kinetic analysis of the active site Glu177 of ricin A-chain, *Protein Eng*. 6, 425-31.
21. Jolliffe, N. A., Di Cola, A., Marsden, C. J., Lord, J. M., Ceriotti, A., Frigerio, L. & Roberts, L. M. (2006) The N-terminal ricin propeptide influences the fate of ricin A-chain in tobacco protoplasts, *J Biol Chem*. 281, 23377-85.
22. Weston, S. A., Tucker, A. D., Thatcher, D. R., Derbyshire, D. J. & Pauptit, R. A. (1994) X-ray structure of recombinant ricin A-chain at 1.8 Å resolution, *J Mol Biol*. 244, 410-22.
23. Hazes, B. & Read, R. J. (1997) Accumulating evidence suggests that several AB-toxins subvert the endoplasmic reticulum-associated protein degradation pathway to enter target cells, *Biochemistry*. 36, 11051-4.
24. Herruer, M. H., Mager, W. H., Raue, H. A., Vreken, P., Wilms, E. & Planta, R. J. (1988) Mild temperature shock affects transcription of yeast ribosomal protein genes as well as the stability of their mRNAs, *Nucleic Acids Res*. 16, 7917-29.
25. Li, B., Nierras, C. R. & Warner, J. R. (1999) Transcriptional elements involved in the repression of ribosomal protein synthesis, *Mol Cell Biol*. 19, 5393-404.
26. Di Cola, A., Frigerio, L., Lord, J. M., Roberts, L. M. & Ceriotti, A. (2005) Endoplasmic reticulum-associated degradation of ricin A chain has unique and plant-specific features, *Plant Physiol*. 137, 287-96.
27. Sikorski, R. S. & Hieter, P. (1989) A system of shuttle vectors and yeast host strains designed for efficient manipulation of DNA in *Saccharomyces cerevisiae*, *Genetics*. 122, 19-27.
28. Gietz, R. D. & Woods, R. A. (2002) Transformation of yeast by lithium acetate/single-stranded carrier DNA/polyethylene glycol method, *Methods Enzymol*. 350, 87-96.
29. Sambrook, J., Fritsch, E. F. & Maniatis, T. (1989) *Molecular Cloning: a laboratory manual*, 2nd edn, Cold Spring Harbor Laboratory Press.
30. Hoffman, C. S. & Winston, F. (1987) A ten-minute DNA preparation from yeast efficiently releases autonomous plasmids for transformation of *Escherichia coli*, *Gene*. 57, 267-72.
31. Marsden, C. J., Fulop, V., Day, P. J. & Lord, J. M. (2004) The effect of mutations surrounding and within the active site on the catalytic activity of ricin A chain, *Eur J Biochem*. 271, 153-62.

32. Ready, M. P., Kim, Y. & Robertus, J. D. (1991) Site-directed mutagenesis of ricin A-chain and implications for the mechanism of action, *Proteins*. *10*, 270-8.
33. Otwinowski, Z. & Minor, W. (1997) Processing of X-ray diffraction data collected in oscillation mode. , *Methods in Enzymology*. *276*, 307–326.
34. Murshudov, G. N., Vagin, A. A. & Dodson, E. J. (1997) Refinement of macromolecular structures by the maximum-likelihood method, *Acta Crystallogr D Biol Crystallogr*. *53*, 240-55.
35. Jones, T. A., Zou, J. Y., Cowan, S. W. & Kjeldgaard, M. (1991) Improved methods for building protein models in electron density maps and the location of errors in these models, *Acta Crystallogr A*. *47 (Pt 2)*, 110-9.
36. Perrakis, A., Sixma, T. K., Wilson, K. S. & Lamzin, V. S. (1997) wARP: improvement and extension of crystallographic phases by weighted averaging of multiple-refined dummy atomic models, *Acta Crystallogr D Biol Crystallogr*. *53*, 448-55.
37. Schmitt, M. E., Brown, T. A. & Trumppower, B. L. (1990) A rapid and simple method for preparation of RNA from *Saccharomyces cerevisiae*, *Nucleic Acids Res*. *18*, 3091-2.
38. Kirby, K. S. (1968) Isolation of nucleic acids with phenolic solvents., *Methods in Enzymology*. *XIIB*, 87-100.
39. Brunger, A. T. (1992) Free R. value: a novel statistical quantity for assessing the accuracy of crystal structures., *Nature*. *355*, 472–474.
40. Read, R. J. (1986) Improved Fourier coefficients for maps using phases from partial structures with errors., *Acta Crystallog.* , 140–149.
41. Kraulis, P. J. (1991) MOLSCRIPT: a program to produce both detailed and schematic plots of protein structures., *J Appl Crystallog.* *24*, 946–950.
42. Esnouf, R. M. (1997) An extensively modified version of MolScript that includes greatly enhanced coloring capabilities. , *J Mol Graph Model*. *15*, 132–134.

Table I

Data collection and refinement statistics		
	E177D with acetate bound	E177D
Data collection		
Radiation, detector and wavelength (Å)	ESRF, ID14-1 MAR CCD, 0.934	MAXLAB BL-I711 MAR IP, 1.0213
Unit cell dimensions (Å)	$a=b=67.7, c=141.2$	$a=b=67.4, c=140.7$
Resolution (Å)	28 - 1.6 (1.66 - 1.6)	30 - 1.39 (1.44 - 1.39)
Observations	243,770	241,261
Unique reflections	43,856	60,577
$I/\sigma(I)$	42.8 (9.5)	41.6 (6.8)
R_{sym}^a	0.042 (0.078)	0.033 (0.114)
Completeness (%)	99.2 (96.3)	91.6 (82.2)
Refinement		
Non-hydrogen atoms	2,559 (including 2 sulfate, 1 acetate and 467 water molecules)	2,586 (including 2 sulfate, 1 glycerol and 492 water molecules)
R_{cryst}^b	0.175 (0.323)	0.173 (0.210)
Reflections used	42,077 (2928)	58,150 (3,884)
R_{free}^c	0.209 (0.372)	0.197 (0.255)
Reflections used	1,799 (108)	2,448 (170)
R_{cryst} (all data) ^b	0.177	0.174
Mean temperature factor (Å ²)	19.3	17.8
Rmsds from ideal values		
Bonds (Å)	0.017	0.014
Angles (°)	1.5	1.6
DPI coordinate error (Å)	0.081	0.058
PDB accession codes	Will be provided	Will be provided

Numbers in parentheses refer to values in the highest resolution shell.

^a $R_{\text{sym}} = \sum_j \sum_h |I_{h,j} - \langle I_h \rangle| / \sum_j \sum_h \langle I_h \rangle$ where $I_{h,j}$ is the j th observation of reflection h , and $\langle I_h \rangle$ is the mean intensity of that reflection.

^b $R_{\text{cryst}} = \sum ||F_{\text{obs}}| - |F_{\text{calc}}|| / \sum |F_{\text{obs}}|$ where F_{obs} and F_{calc} are the observed and calculated structure factor amplitudes, respectively.

^c R_{free} is equivalent to R_{cryst} for a 4 % subset of reflections not used in the refinement [39].

Figure Legends

Fig. 1. Schematic showing the principle of generating temperature-dependent toxin A chains. A gap repair protocol was used to generate RTA DNA mutated as described previously [15]. RTA ORFs containing mutations that attenuate activity are depicted as RTA*. These were co-transformed with a plasmid containing a wild-type RTA sequence cut within the coding region. Transformants were selected on the basis of a nutritional marker (*URA3* gene), contained within the vector, and by the ability of cells to recombine the two DNA molecules by gap repair. Transformed cells were plated at either 23°C or 37°C depending on temperature-variant required, before being replica plated at 37°C and 23°C respectively.

Fig. 2. Phenotypic analysis of RTA mutants. (A) Mutations discovered in the RTA ORFs of survivors recovered from the screen depicted in Fig. 1 were re-made as single and/or as double mutations and subsequent viabilities of transformed yeast cells were analyzed. As controls, the known inactive toxin (Kar2_{SP}-RTA Δ) and wild-type toxin (Kar2_{SP}-RTA), were included. (B) Yeast cells were transformed with plasmids that encode cytosolic versions of either the inactive RTA Δ , native RTA or RTA_{F108L/L151P}, plated at the indicated temperatures and left for three days.

Fig. 3. Growth and viabilities of the conditional ricin A chain mutants. (A) Transformed yeast cells were grown in liquid media at permissive temperatures (30°C for Kar2_{SP}-RTA Δ and Kar2_{SP}-RTA_{E177D}; 37°C for Kar2_{SP}-RTA_{F108L/L151P}) before dilution and plating at 1×10^4 cells per plate. Plates were incubated at the respective temperature for the time

shown to permit growth of similar size colonies. (B) Growth assays in liquid medium of cells transformed with Kar2_{SP}-RTA_{E177D} and Kar2_{SP}-RTA_{F108L/L151P} are shown. Closed squares represent growth of Kar2_{SP}-RTA_{E177D} at 30°C; open squares represent growth of Kar2_{SP}-RTA_{E177D} at 37°C; closed triangles represent growth of Kar2_{SP}-RTA_{F108L/L151P} at 37°C; open triangles represent growth of Kar2_{SP}-RTA_{F108L/L151P} at 23°C. (C) Cell viabilities. Cells that had been expressing Kar2_{SP}-RTA_{E177D} and Kar2_{SP}-RTA_{F108L/L151P} at non-permissive temperatures (in B) were plated onto selective medium and grown at the temperature permissive for growth for 48 hours. Open squares represent growth of Kar2_{SP}-RTA_{E177D} expressing cells at 37°C; open triangles represent growth of Kar2_{SP}-RTA_{F108L/L151P} cells at 23°C. The graph represents the percentage of viable cells after plating.

Fig. 4. Growth of yeast is attenuated at non-permissive temperatures because of toxin-mediated damage to ribosomes. rRNAs were isolated from 5×10^7 yeast cells expressing Kar2_{SP}-RTA_{E177D} and Kar2_{SP}-RTA_{F108L/L151P} grown at different temperatures. These were treated with acetic-aniline and resolved on denaturing gels that were then blotted for the rRNA fragment liberated from 25S rRNA following toxin-mediated damage *in vivo*. Percentage depurination was determined by quantifying the intensity of the liberated fragment in relation to the remaining intact 25S rRNA plus fragment using TotalLab™ version 2003.02, Non-linear Dynamics Ltd. (A) Percentage of depurinated rRNA at zero and 24 hours from cells expressing Kar2_{SP}-RTA_{E177D} or (B) Kar2_{SP}-RTA_{F108L/L151P}, at the different temperatures. Results shown are the averages of duplicate determinations of three independent isolates (\pm SD).

Fig. 5. Ricin A chain mutants are targeted and processed within the yeast endoplasmic reticulum. Transformed yeast expressing either, Kar2_{SP}-RTA Δ , Kar2_{SP}-RTA_{E177D} or Kar2_{SP}-RTA_{F108L/L151P} was grown at respective permissive temperatures. Cells were radiolabeled for 20 minutes with [³⁵S]-ProMix, RTA immunoprecipitated and either treated with (+) or without (-) endoglycosidase H to determine the presence and extent of *N*-linked glycosylation. As size controls, *in vitro* translations of mature RTA and Kar2_{SP}-RTA are shown for comparison. Products were analyzed by SDS-PAGE and visualised by fluorography. g0 refers to non glycosylated RTA, g1 refers to a singly glycosylated RTA and g2 a doubly glycosylated RTA.

Fig. 6. Stability of mutant ricin A chains. The kinetics of protein degradation of (A) Kar2_{SP}-RTA_{E177D} and (B) Kar2_{SP}-RTA_{F108L/L151P} at all temperatures, or a cytosolic version (cRTA_{F108L/L151P}) at 37°C, was visualised following pulse-chase of the respective RTA expressed in transformed cells. Cells were grown at the temperatures permissive for growth before a 20 minute pulse with [³⁵S]-ProMix at different temperatures. Chase samples were taken at zero, 10, 20 and 30 minutes prior to immunoprecipitation and gel analysis.

Fig. 7. Catalytic activity of RTA_{E177D} at different temperatures. (A) Purified RTA_{E177D} was incubated with salt-washed yeast ribosomes for 60 minutes at either 30°C or 37°C at concentrations from 250 ng/ μ l in halving dilutions to 1.95 ng/ μ l. A control, at the highest concentration of RTA_{E177D}, was included that was not subsequently treated with the aniline reagent. Total rRNA was then isolated from extracted ribosomes and 4 μ g samples

treated with acetic-aniline pH 4.5 for 2 minutes at 60°C. Samples were electrophoresed on a denaturing agarose/formamide gel. (B) The fragments released by aniline (marked by arrowheads) were quantified by densitometry using TotalLab™, version 2003.02, Nonlinear Dynamics Ltd and plotted. Squares represent growth of cells expressing Kar2_{SP}-RTA_{E177D} at 37°C; circles represent growth of Kar2_{SP}-RTA_{E177D} at 30°C;

Fig. 8. Three dimensional structure of RTA_{E177D}. (A) and (B) Electron density of RTA_{E177D} in the vicinity of the active site, with and without bound acetate, respectively. The SIGMAA [40] weighted 2mFo-DFc electron density using phases from the final model is contoured at 1 σ level, where σ represents the rms electron density for the unit cell. Contours more than 1.4 Å. from any of the displayed atoms have been removed for clarity. Drawn with MOLSCRIPT [41, 42]. (C) Close view of the active site of the wild type enzyme, drawn from PDB entry 1ift. (D) Ribbon diagram showing key amino acids. The active site molecules Y80, Y123 and E177 are shown in green and the position of the two mutated amino acids, F108 and L151, are shown in blue.

Figure 1.

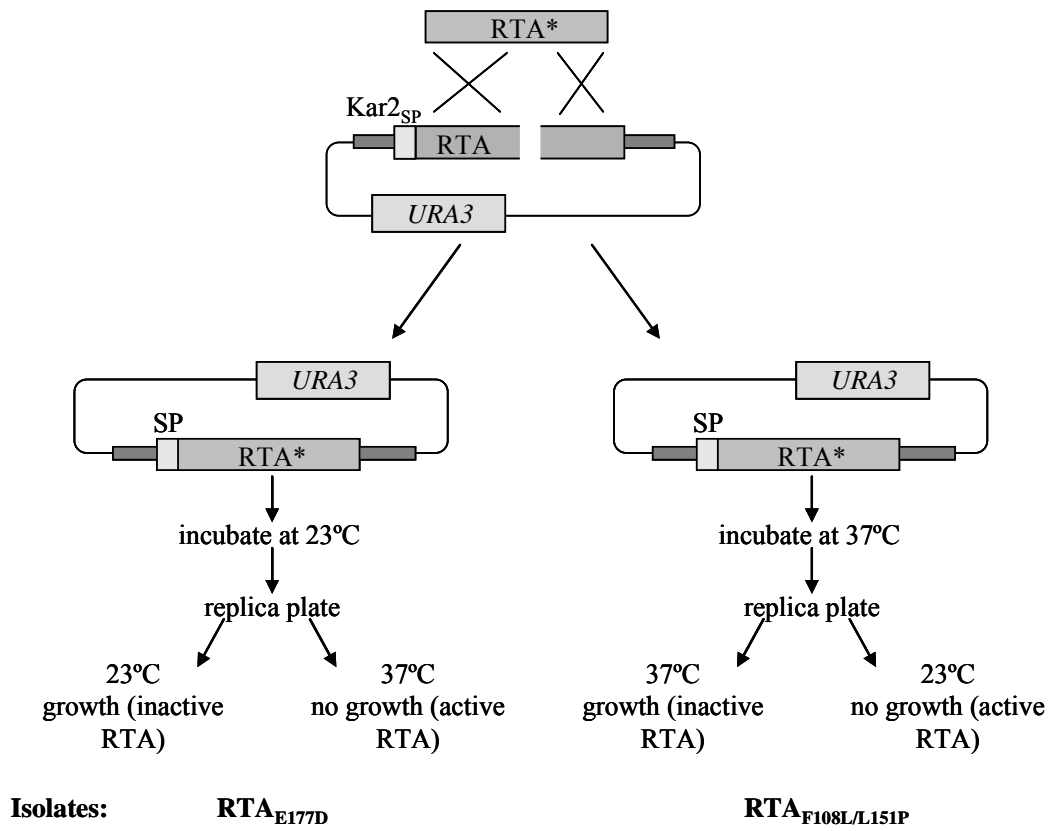


Figure 2.

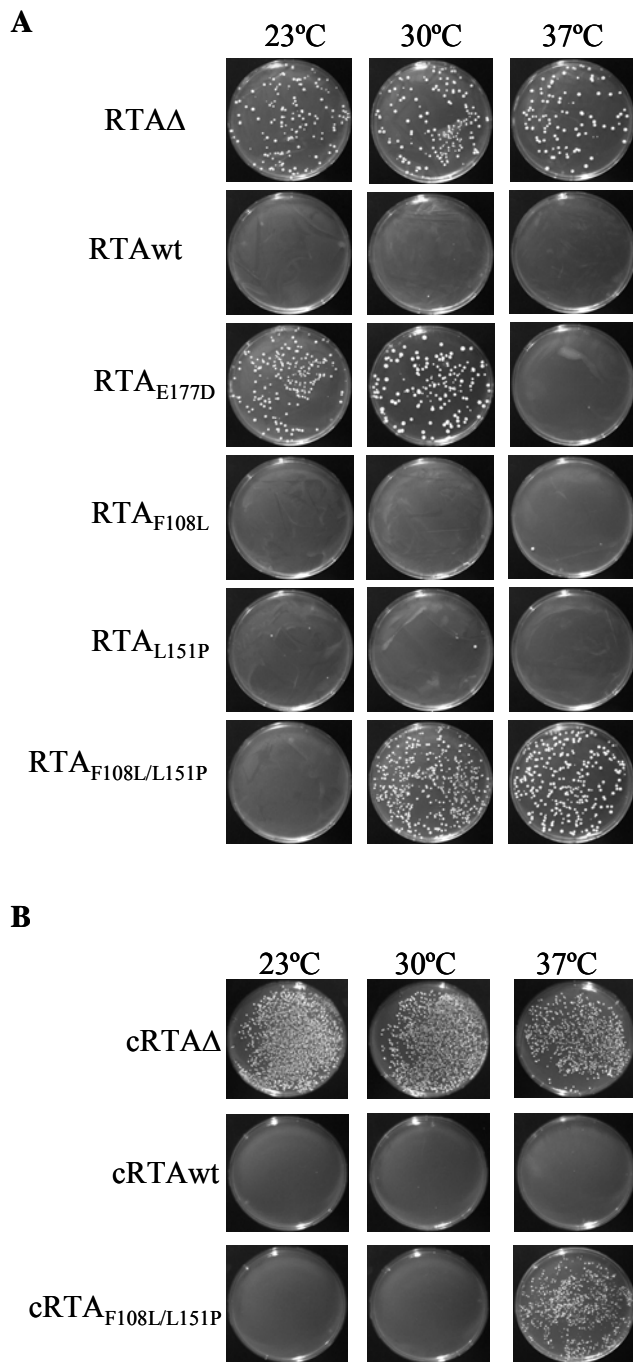


Figure 3.

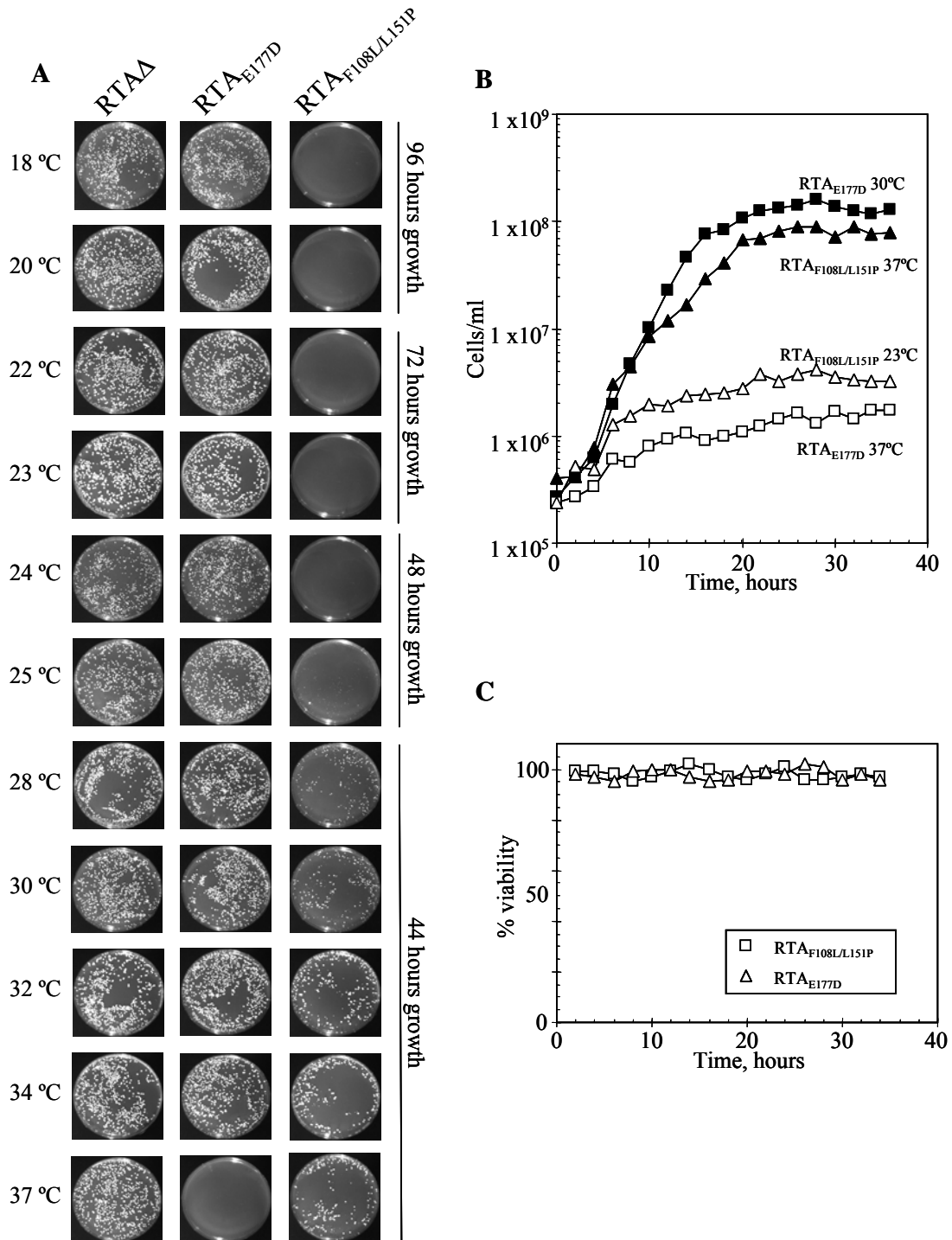
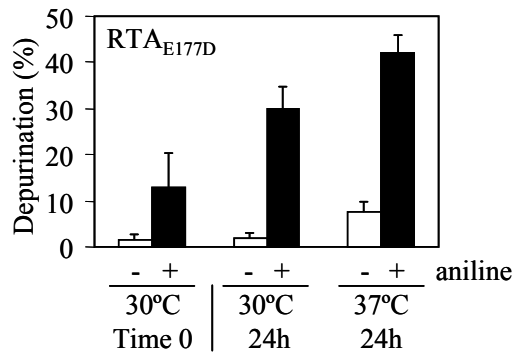


Figure 4.

A



B

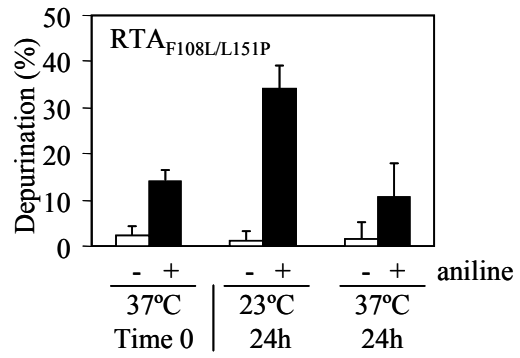


Figure 6.

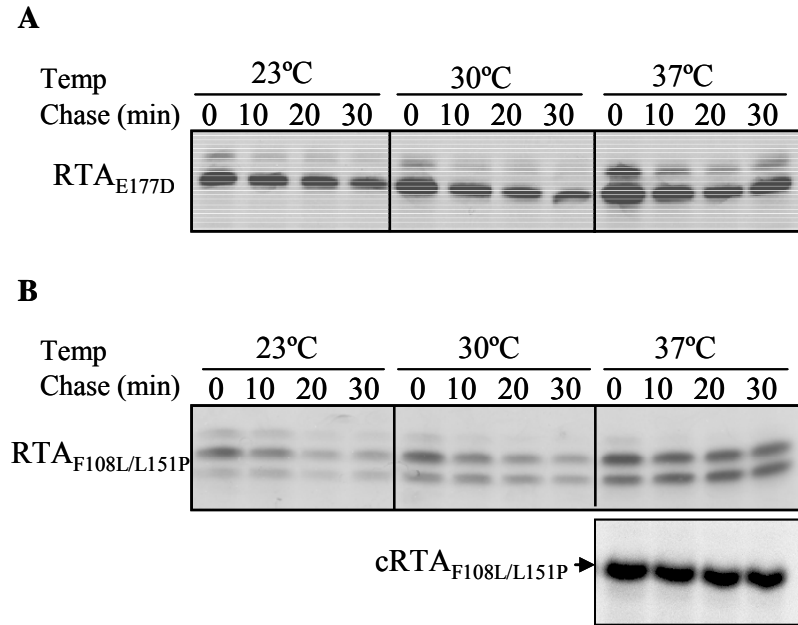


Figure 7.

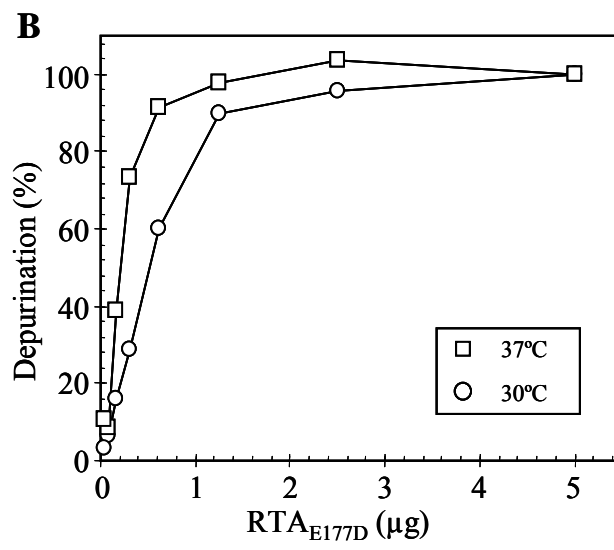
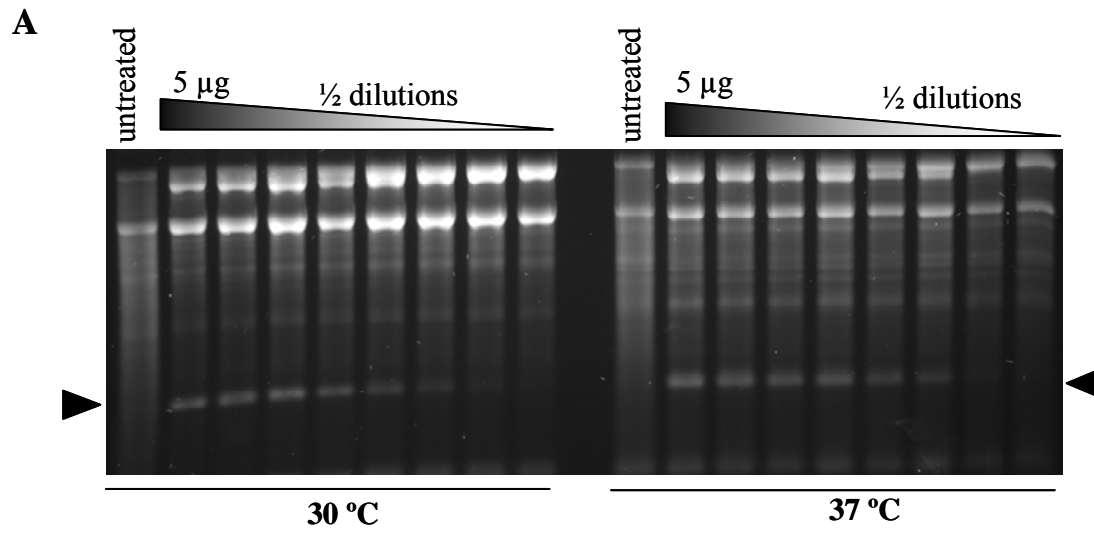
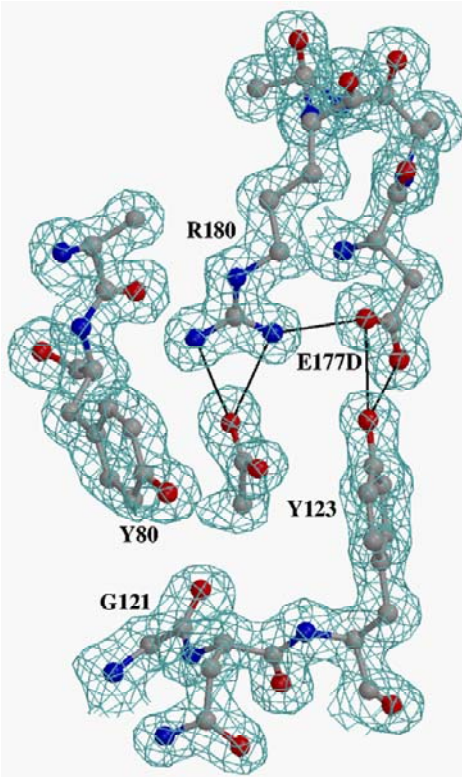
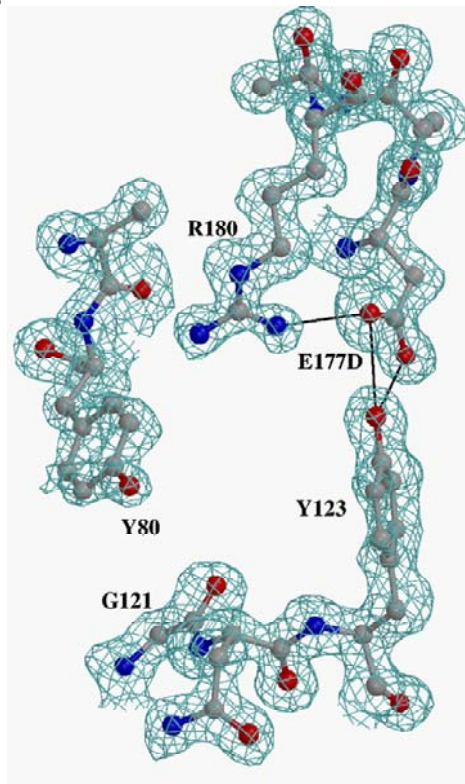


Figure 8.

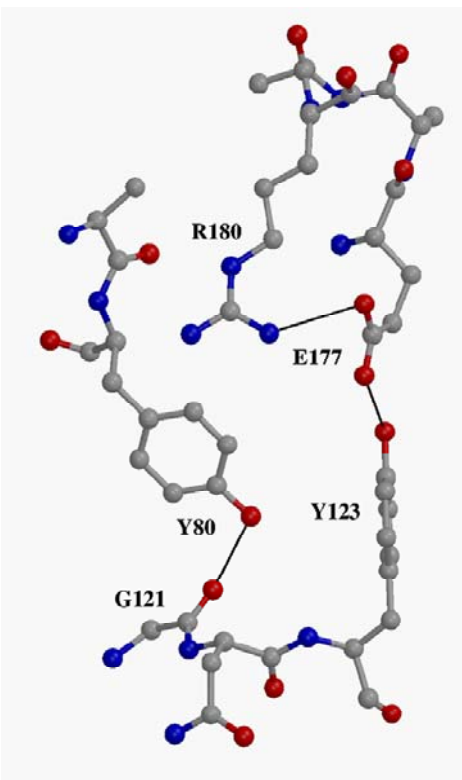
A



B



C



D

